402-02-005 ISMRM ABSTRACT

Low Rank Motion Correction for IVIM and Diffusion Spectrum Quantification for Indeterminate Renal Masses

Primary: Diffusion - IVIM 〉 **Secondary:** Body - Kidney 〉 **Oral** · 11 min | Inside the Bean: Advances in Renal MRI · Tuesday, 12 May, 9:04 AM–9:15 AM · Session: 8:20–10:10 AM · Hall 1B 〉 **Keywords:** KIDNEY IVIM MOTION CORRECTION APPARENT DIFFUSION COEFFICIENT LOW RANK

Ningjun Wang [1], **Michael J Jaroszewicz**[1], **Yun Jiang**[1,2], **Zhengguo Tan**[1], **Jesse Hamilton**[1,2], **Vikas Gulani**[1], **Hero K Hussain**[1], **Matthew Davenport**[1,3], **Nicole Seiberlich**[1,2], **Gastao Cruz**[1]

[1]Department of Radiology, University of Michigan, Ann Arbor, United States of America
[2]Department of Biomedical Engineering, University of Michigan, Ann Arbor, United States of America
[3]Department of Urology, University of Michigan, Ann Arbor, United States of America

Presenting Author: *Ningjun Wang (wnjjacky@umich.edu)*

Impact

IVIM and diffusion spectrum quantification using a fast free-breathing diffusion EPI protocol is feasible in healthy subjects and renal mass patients. This type of quantitative diffusion data could help in the characterization of indeterminate renal masses.

Synopsis

Motivation: IVIM and diffusion spectrum quantification have the potential to characterize kidney tissue. However, they require images with different b-values, typically acquired free-breathing, making them motion-sensitive and prone to noise/aliasing.

Goals: Investigate the feasibility of IVIM and diffusion spectrum quantification in indeterminate renal masses using a novel Low Rank Motion Corrected reconstruction.

Approach: Multi-slice, single-shot EPI with 50 b-values was acquired free-breathing and reconstructed with LRMC^{H}-DP to fit ADC, IVIM and diffusion spectrum.

Results: Compared to SENSE, LRMC^{H}-DP reduced motion artefacts/noise in IVIM maps and provided more stable diffusion spectra, consistent with ADC and IVIM findings. Results show distinct spectra in different renal tissues.

Introduction

Indeterminate renal masses are clinically assessed with a combination of pre-contrast T2-weighted, pre-/post-contrast T1-weighted, and diffusion-weighted (including Apparent Diffusion Coefficient, ADC) imaging. Intra-voxel incoherent-motion (IVIM)[1] considers a bi-exponential model, capable of measuring both diffusion (D) and perfusion (D*), as well as the fraction between them (PF), and has been used to grade clear cell renal cell carcinoma.[2] The complementary information from other multi-exponential diffusion models has also been used to characterize solid renal masses,[3] suggesting that further diagnostic information may be found in the full quantitative diffusion spectrum. However, mapping the diffusion spectrum requires a large number of b-value data, and consequently accelerated, free-breathing protocols. In this study, we present a free-breathing, low-rank, motion-corrected reconstruction framework and investigate its feasibility of quantifying ADC, IVIM, and spectral diffusion in renal masses.

Methods

Diffusion data were acquired with multi-slice, single-shot free-breathing EPI. Low Rank Motion Correction (LRMC)[4] was combined with Virtual Coil Concept (VCC)[5] and Dictionary-Patch based regularization (DP)[6] to perform respiratory motion correction and suppress residual aliasing/noise artefacts (Fig. 1). First, a preliminary SENSE[7] reconstruction was performed to estimate image phase, voxel-wise low rank subspaces of diffusion via SVD of local Casorati matrices, and respiratory motion via image registration using NiftyReg[8, 9]. Secondly, data were reconstructed using LRMC^{H}-DP as shown in Fig. 1. Finally, reconstructed data were fitted using i) a single exponential fit for ADC, ii) a bi-exponential fit for IVIM[12] (diffusion D, perfusion D* and perfusion fraction PF) and iii) sparse non-negative least squares fit to map the full diffusion spectrum G(D). An in-house built diffusion phantom, three healthy subjects and four patients referred for indeterminate renal masses were scanned at 1.5T (Magnetom Sola, Siemens Healthineers, Erlangen, Germany) with a free-breathing, multi-slice single-shot EPI. Imaging settings included: FOV=400x400 mm^2; resolution=1.6×1.6 mm^2; TE/TR=105/8700 ms; 5/8 Partial Fourier; 20 slices; 50 b-values with 30 b-values between [0 – 200] s/mm^2 and 20 b-values between [200 – 1400] s/mm^2; ~8-minute scan time. Data was reconstructed using SENSE and LRMC^{H}-DP, and fitted for ADC, IVIM and diffusion spectrum. Regions of interest were delineated on the renal cortex and medulla for all subjects and renal masses in patients to calculate the mean and standard deviation for ADC, D, D*, and PF.

Results

The proposed approach was validated on a phantom, where fitted ADC values showed excellent linear correlation with a R^2~0.99 with ground-truth values (Fig. 2a). Multiple cysts with high D (2.86×10^{-3}) and negligeable PF (~0%) were observed, as well as a Bosniak IV with lower D (1.63×10^{-3}) and higher D* (1.50×10^{-2}) and PF (32%) in its solid component in patient 1 (Fig. 2b and Fig. 3). Motion and misalignment between b-value images produce motion artefacts in the SENSE D, D* and PF maps, causing a cyst to be mismapped (Fig. 3, patient 2); these are reduced with the proposed approach. Diffusion spectrum G(D) quantification was in agreement with ADC and IVIM measurements. This analysis revealed different spectra in cortex, medulla, and Bosniak IV (cystic/solid components) (Fig. 4). G(D) in kidney parenchyma was in general agreement with previous literature; higher perfusion peaks were observed in the Bosniak IV component, as expected due to its vascularization[13]. The ADC/IVIM measurements were in agreement with literature values[14], and reduced aliasing in LRMC^{H}-DP yielded lower standard deviations relative to SENSE for all diffusion parameters (Fig. 2b). The cumulative diffusion spectrum is shown in Fig. 5, depicting the accrued diffusion along G(D). Slow diffusion is present in both renal parenchyma and Bosniak IV (solid), followed by slightly faster diffusion occurring in cysts, and finally fast perfusion in the Bosniak IV (solid) and highly vascular regions of the renal parenchyma.

Discussion

Preliminary results indicate that the proposed LRMC^{H}-DP method suppresses noise and motion artefacts present in conventional SENSE reconstructions, ensuring better quality data prior to model fitting in quantitative diffusion. The main slow component of the diffusion spectrum is highly consistent with the fitted D value, although some differences were observed in the measured PFs. Distinct spectra were observed in different renal masses. While these in vivo patient findings are preliminary, they represent a promising step and suggest the potential of this technique for clinical renal mass characterization.

Conclusion

We demonstrated a robust LRMC^{H}-DP framework for feasible, free-breathing, motion-corrected quantitative diffusion mapping. Using this method, diffusion spectrum quantification was shown to be in agreement with IVIM and ADC measurements and was capable of revealing distinct diffusion profiles in Bosniak IV renal masses.

Acknowledgements

This work was supported in part by the NIH (R01 HL153034, R01HL163991, R01HL163030) and Siemens Healthineers.

References

1. Le Bihan D, Breton E, Lallemand D, Aubin ML, Vignaud J, Laval-Jeantet M. Separation of diffusion and perfusion in intravoxel incoherent motion MR imaging. Radiology. 1988 Aug;168(2):497–505.

2. Zhu Q, Zhu W, Wu J, Chen W, Ye J, Ling J. Comparative study of conventional diffusion-weighted imaging and introvoxel incoherent motion in assessment of pathological grade of clear cell renal cell carcinoma. The British Journal of Radiology [Internet]. 2022 May 1 [cited 2023 May 10];95(1133). Available from: https://doi.org/10.1259/bjr.20210485

3. van Baalen S, Froeling M, Asselman M, Klazen C, Jeltes C, van Dijk L, et al. Mono, bi- and tri-exponential diffusion MRI modelling for renal solid masses and comparison with histopathological findings. Cancer Imaging [Internet]. 2018 Nov 26 [cited 2022 Oct 5];18(1). Available from: https://doi.org/10.1186/s40644-018-0178-0

4. Cruz G, Qi H, Jaubert O, Küstner T, Schneider T, Botnar RM, et al. Generalized low-rank nonrigid motion-corrected reconstruction for MR fingerprinting. Magnetic Resonance in Medicine [Internet]. 2021 Oct 2 [cited 2023 Jul 13];87(2):746–63. Available from: https://doi.org/10.1002/mrm.29027

5. Blaimer M, Gutberlet M, Kellman P, Breuer FA, Köstler H, Griswold MA. Virtual coil concept for improved parallel MRI employing conjugate symmetric signals. Magnetic Resonance in Medicine [Internet]. 2008 Dec 18 [cited 2023 Mar 10];61(1):93–102. Available from: https://doi.org/10.1002/mrm.21652

6. Cruz G, Cummings E, Griesler T, Hamilton J, Vikas Gulani, Davenport M, et al. 3D Free-breathing T1, T2, T2* and PDFF mapping in the kidneys with Dictionary-Patch regularized Low Rank Motion Corrected Rosette MRF. Proceedings on CD-ROM - International Society for Magnetic Resonance in Medicine Scientific Meeting and Exhibition/Proceedings of the International Society for Magnetic Resonance in Medicine, Scientific Meeting and Exhibition [Internet]. 2025 Sep 16 [cited 2025 Oct 27]; Available from: https://doi.org/10.58530/2025/2733

7. Pruessmann KP, Weiger M, Börnert P, Boesiger P. Advances in sensitivity encoding with arbitraryk-space trajectories. Magnetic Resonance in Medicine [Internet]. 2001 Oct [cited 2020 Mar 24];46(4):638–51. Available from: https://doi.org/10.1002/mrm.1241

8. Rueckert D, Sonoda LI, Hayes C, Hill DLG, Leach MO, Hawkes DJ. Nonrigid registration using free-form deformations: application to breast MR images. IEEE Transactions on Medical Imaging [Internet]. 1999 [cited 2020 Jun 10];18(8):712–21. Available from: https://doi.org/10.1109/42.796284

9. Modat M, Ridgway GR, Taylor ZA, Lehmann M, Barnes J, Hawkes DJ, et al. Fast free-form deformation using graphics processing units. Computer Methods and Programs in Biomedicine [Internet]. 2010 Jun [cited 2021 Apr 16];98(3):278–84. Available from: https://doi.org/10.1016/j.cmpb.2009.09.002

10. Mehmet Akçakaya, Basha T, Goddu B, Goepfert L, Kissinger KV, Vahid Tarokh, et al. Low-dimensional-structure self-learning and thresholding: Regularization beyond compressed sensing for MRI Reconstruction. Magnetic Resonance in Medicine [Internet]. 2011 Apr 4 [cited 2023 Dec 8];66(3):756–67. Available from: https://doi.org/10.1002/mrm.22841

11. Bustin A, Lima da Cruz G, Jaubert O, Lopez K, Botnar RM, Prieto C. High-dimensionality undersampled patch-based reconstruction (HD-PROST) for accelerated multi-contrast MRI. Magnetic Resonance in Medicine [Internet]. 2019 Jun 1 [cited 2023 Feb 28];81(6):3705–19. Available from: https://pubmed.ncbi.nlm.nih.gov/30834594/ [pmid]

12. Jalnefjord O, Andersson M, Montelius M, Starck G, Elf AK, Johanson V, et al. Comparison of methods for estimation of the intravoxel incoherent motion (IVIM) diffusion coefficient (D) and perfusion fraction (f). Magnetic Resonance Materials in Physics Biology and Medicine [Internet]. 2018 Aug 16 [cited 2025 Oct 27];31(6):715–23. Available from: https://doi.org/10.1007/s10334-018-0697-5

13. Liu M, Dyke J, Gladytz T, Jasse J, Bolger I, Calle S, et al. Spectral diffusion MRI detects early fibrosis in renal allografts in a pilot clinical translational study. ISMRM Annual Meeting [Internet]. [cited 2025 Oct 29]; Available from: https://doi.org/10.58530/2025/1020

14. Bane O, Wagner M, Zhang JL, Dyvorne HA, Orton M, Rusinek H, et al. Assessment of renal function using intravoxel incoherent motion diffusion-weighted imaging and dynamic contrast-enhanced MRI. Journal of Magnetic Resonance Imaging [Internet]. 2016 Feb 8 [cited 2025 Mar 16];44(2):317–26. Available from: https://doi.org/10.1002/jmri.25171

Figures and Tables

Fig. 1

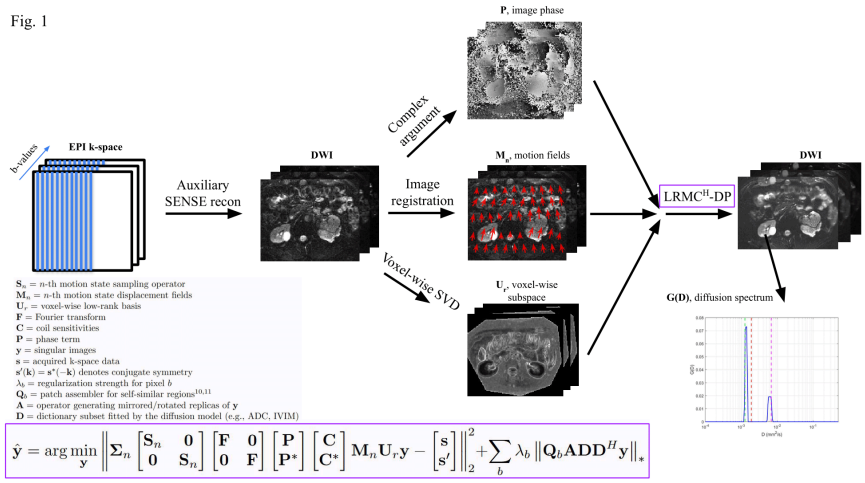

Scan for high-resolution version

Figure 1: *Figure 1. Framework for the proposed LRMC^H-DP reconstruction. Initial DWIs from a preliminary SENSE reconstruction are processed to estimate voxel-wise low-rank subspaces (**U**$_r$) and motion fields (**M**$_n$). These components, along with image phase (**P**), are incorporated into the LRMC^H-DP optimization (formula shown) to yield the final motion-corrected DWI, from which the diffusion spectrum G(D) is derived.*

Fig. 2

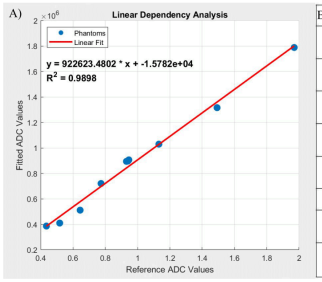

B) Table 1

Metrics	SENSE ADC (×10^{-3})	SENSE D (×10^{-3})	SENSE D* (×10^{-2})	SENSE PF	LRMC^H-DP ADC (×10^{-3})	LRMC^H-DP D (×10^{-3})	LRMC^H-DP D* (×10^{-2})	LRMC^H-DP PF
Healthy Cortex	1.75±0.30	1.30±0.40	1.17±1.56	0.29±0.17	1.62±0.20	1.35±0.35	0.92±0.60	0.28±0.13
Healthy Medulla	1.73±0.28	1.38±0.26	1.42±2.15	0.26±0.12	1.61±0.18	1.38±0.16	0.92±0.72	0.27±0.09
Patient Cortex	1.82±0.59	1.22±0.72	1.45±2.25	0.35±0.21	1.55±0.57	1.25±0.67	1.25±1.68	0.37±0.16
Patient Medulla	1.77±0.63	1.20±0.74	1.90±2.65	0.33±0.19	1.50±0.61	1.25±0.68	1.75±2.46	0.33±0.14
Cyst	2.93±0.25	2.83±0.18	6.66±4.34	0.10±0.16	2.77±0.09	2.86±0.08	8.46±3.76	0.00±0.00
Bosniak IV (Cystic)	3.21±0.28	2.80±0.28	0.62±1.22	0.16±0.20	3.00±0.13	2.86±0.18	0.87±1.17	0.15±0.16
Bosniak IV (Solid)	1.74±0.21	1.48±0.26	2.65±2.56	0.37±0.15	1.79±0.08	1.63±0.09	1.50±0.18	0.32±0.03

Scan for high-resolution version

Figure 2: *Figure 2. Quantitative validation of the LRMC^H-DP method. A) Linear dependency plot shows high accuracy (R^2=0.9898) between fitted ADC values and ground-truth reference values in a diffusion phantom. B) Table 1 compares IVIM parameters from SENSE and LRMC^H-DP in tissues, which values agree with literature. LRMC^H-DP shows lower standard deviations, indicating improved fitting stability.*

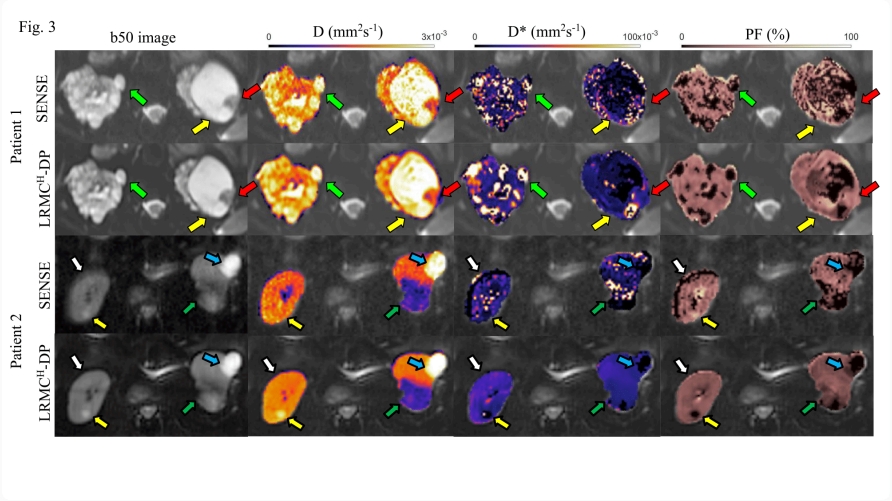

Scan for high-resolution version

Figure 3: *Figure 3. LRMC^H-DP and SENSE reconstructions of IVIM parameter maps (b50, D, D*, PF) in two patients referred for indeterminate renal masses. The LRMC^H-DP method demonstrates reduced noise and greater homogeneity. Arrow key: (Patient 1) green=cyst, yellow=cystic component (Bosniak IV), red=solid compartment; (Patient 2) yellow=cyst, blue=Bosniak II, green=hematoma.*

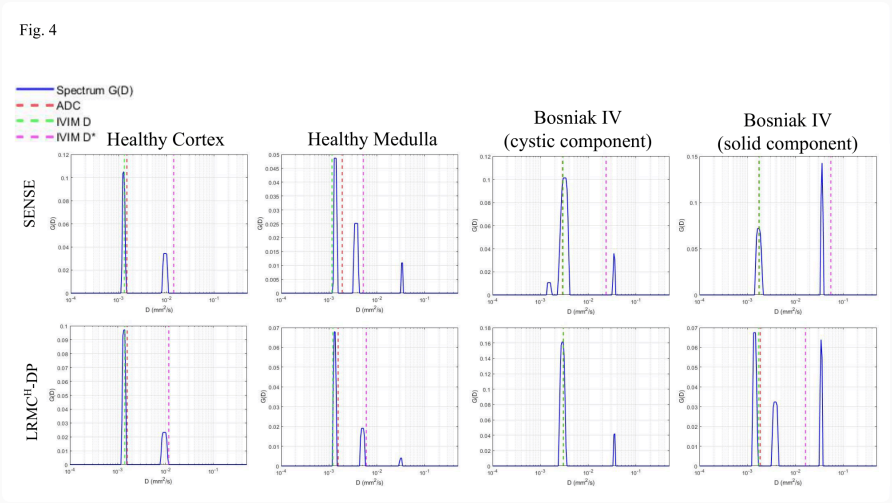

Scan for high-resolution version

Figure 4: *Figure 4. Diffusion spectra for healthy kidney and renal mass tissues using SENSE vs. LRMC^H-DP. LRMC^H-DP demonstrates more stable and better-fitted peaks across all tissues, including the Bosniak IV mass. Reference lines: ADC (red), IVIM D (green), and D* (pink).*

Animated Figure 5

This figure contains animation/video content. To view the animation, scan the QR code with your mobile device or visit the online version of this abstract.

Figure 5: *Figure 5. Visualization of the cumulative G(D) in two representative kidney slices. This metric is the cumulative sum of the diffusion spectrum G(D) components up to the D-value (x-axis). The image shows signal build-up, where increases in brightness correspond to diffusion peaks, showing how the signal builds up from slow to fast diffusion in different tissues. For example, cysts show one main jump, while Bosniak IV solid components show their main jump at higher D-values.*